Stem Cell Reports
Article

ISSCR

OPEN ACCESS

Human iPSC-Derived Hepatocyte-like Cells Support *Plasmodium* Liver-Stage Infection In Vitro

Shengyong Ng,[1] Robert E. Schwartz,[2,3] Sandra March,[2,6] Ani Galstian,[2,6] Nil Gural,[2] Jing Shan,[2] Mythili Prabhu,[2] Maria M. Mota,[4,5] and Sangeeta N. Bhatia[2,3,5,6,*]

[1]Department of Biological Engineering, Massachusetts Institute of Technology, Cambridge, MA 02139, USA
[2]Health Sciences and Technology/Institute for Medical Engineering and Science, Massachusetts Institute of Technology, Cambridge, MA 02139, USA
[3]Department of Medicine, Brigham and Women's Hospital, Boston, MA 02115, USA
[4]Unidade de Malária, Instituto de Medicina Molecular, Universidade de Lisboa, 1649-028 Lisboa, Portugal
[5]Howard Hughes Medical Institute, Koch Institute, and Electrical Engineering and Computer Science, Massachusetts Institute of Technology, Cambridge, MA 02139, USA
[6]Broad Institute, Cambridge, MA 02139, USA
*Correspondence: sbhatia@mit.edu
http://dx.doi.org/10.1016/j.stemcr.2015.01.002

SUMMARY

Malaria eradication is a major goal in public health but is challenged by relapsing malaria species, expanding drug resistance, and the influence of host genetics on antimalarial drug efficacy. To overcome these hurdles, it is imperative to establish in vitro assays of liver-stage malaria for drug testing. Induced pluripotent stem cells (iPSC) potentially allow the assessment of donor-specific drug responses, and iPSC-derived hepatocyte-like cells (iHLCs) can facilitate the study of host genetics on host-pathogen interactions and the discovery of novel targets for antimalarial drug development. We establish in vitro liver-stage malaria infections in iHLCs using *P. berghei*, *P. yoelii*, *P. falciparum*, and *P. vivax* and show that differentiating cells acquire permissiveness to malaria infection at the hepatoblast stage. We also characterize antimalarial drug metabolism capabilities of iHLCs using prototypical antimalarial drugs and demonstrate that chemical maturation of iHLCs can improve their potential for antimalarial drug testing applications.

INTRODUCTION

Malaria affects 250 million people and causes approximately one million deaths each year (World Health Organization, 2013). As an obligatory stage of the *Plasmodium* life cycle that occurs soon after infection of the human host, the liver stage is an attractive target for the development of antimalarial drugs and vaccines (Mazier et al., 2009; Prudêncio et al., 2006), especially with the goal of malaria eradication. Current in vitro models of liver-stage malaria commonly utilize hepatic cell lines such as HepG2 or HC04 in conjunction with *Plasmodium* sporozoites from either rodent malaria species (*P. berghei*, *P. yoelii)* or human malaria species (*P. falciparum, P. vivax*), which have liver stages that range in length from 2 days for *P. berghei* and *P. yoelii* to 6–8 days for *P. falciparum* and *P. vivax*. Due to their better maintenance of hepatic drug metabolism enzymes compared to hepatic cell lines and the fact that they are the natural host for malarial sporozoites, primary human hepatocytes are a preferable cell type to model liver-stage malaria in vitro for the purposes of antimalarial drug development. These traits of primary human hepatocytes mean they may offer better predictive value in in vitro liver-stage malaria phenotypic drug screens and may more accurately recapitulate host-pathogen interactions in vitro than the cell lines that are typically used for modeling liver-stage malaria (March et al., 2013). However, primary human hepatocytes are sourced from a small pool of donors and thus may not represent the genetic diversity of the human population.

Pluripotent stem cell-derived hepatocytes overcome some of the drawbacks of cell lines, fetal tissue, and adult human sources and may be considered an alternative source of primary human hepatocytes. Compared to primary human hepatocytes, stem cell-derived hepatocytes can represent more diverse genotypes, can be personalized to exhibit rare genotypes, and are renewable in culture. Human pluripotent embryonic stem cells were first isolated from human blastocysts (Thomson, 1998), but embryonic stem cells face considerable ethical issues with regards to their availability and use. More recently, the enforced expression of various factors in a variety of differentiated cell types led to the generation of induced pluripotent stem cells (iPSCs) (Takahashi et al., 2007). In particular, iPSCs can, in a reliable and stepwise manner, differentiate through the developmentally appropriate stages (i.e., endoderm, hepatic specified endoderm, hepatoblasts) to produce hepatocyte-like cells (iHLCs) in vitro (Schwartz et al., 2014). The ability to generate iHLCs from different donors provides an opportunity to assess donor-specific drug responses in vitro, akin to conducting an in vitro clinical trial. Our prior work has shown that iHLCs are susceptible to hepatotropic pathogens such as hepatitis C and hepatitis B virus infection (Schwartz et al., 2012; Shlomai et al., 2014). It remains to be seen whether iHLCs can serve as a host population for liver-stage malaria assays,

especially considering that iHLCs generated using current state of the art protocols are developmentally immature and more closely resemble fetal hepatocytes in their cytochrome P450 expression and activity profiles as well as in their antigen expression (Si-Tayeb et al., 2010). However, recent promising attempts to mature iHLCs to a more adult phenotype, including the identification of small molecules (Shan et al., 2013), genetic manipulation with transduction of a gene for a hepatic transcription factor (Takayama et al., 2012), a combination of 3D culture and cAMP signaling (Ogawa et al., 2013), or in vivo transplantation (Takebe et al., 2013), may ultimately contribute to the generation of appropriately mature iHLCs for antimalarial drug screens, which, to date, have largely been carried out in human hepatoma cells (da Cruz et al., 2012; Derbyshire et al., 2012; Meister et al., 2011). Isogenic iHLCs that are more developmentally mature may also facilitate the discovery of host factors for the *Plasmodium* liver stages.

In this study, we show the feasibility of infecting iHLCs with *Plasmodium* sporozoites in vitro and demonstrate *Plasmodium* parasite development over time in culture. We identify the stage at which cells acquire permissiveness to liver-stage malaria infection during the differentiation process. It is also necessary to characterize the responses of malaria-infected iHLCs to known antimalarial drugs in order to establish the utility of this cell type for use in in vitro liver-stage malaria phenotypic drug screens. We observe that iHLCs are not responsive to the antimalarial drug primaquine and hypothesize this deficiency is due to a lack of bioactivation of the drug by hepatic cytochrome P450 drug metabolism enzymes. Consistent with this model, we further demonstrate that chemically matured iHLCs acquire primaquine sensitivity, highlighting the potential to use iHLCs for antimalarial drug testing.

RESULTS

iPSC-Derived Hepatocyte-like Cells Support Liver-Stage Malaria Infection In Vitro

iPSC-derived hepatocyte-like cells (iHLCs) were generated using a 20 day in vitro differentiation protocol that recapitulates the different stages of hepatic development (Si-Tayeb et al., 2010). During this differentiation process, iPSCs adopt an endoderm fate at 5 days and become hepatic-specified endoderm cells at 10 days, hepatoblasts at 15 days, and iHLCs at 20 days after the initiation of differentiation, respectively (Figure 1A). iHLCs demonstrate typical polygonal hepatocyte morphology (Figure 1B) and express prototypical hepatic markers like human albumin, α1-antitrypsin, and α-fetoprotein (Figure 1C). The two known host entry factors for liver-stage malaria, CD81 and SRB1, are both transcribed and translated in iHLCs (Figures 1D and 1E), and the proteins are appropriately localized on the cell surface, as observed via immunofluorescence assays (Figures 1F and 1G). Based on these observations, we hypothesized that day 20 iHLCs may support *Plasmodium* infection.

Cultures of iHLCs were overlaid with media containing *P. berghei* sporozoites for 3 hr and fixed at 1, 2, or 3 days postexposure. Immunofluorescence assays using antibodies specific for *P. berghei* HSP70 were conducted in order to quantitate iHLC infection by *P. berghei* (Figure 2A). HSP70-expressing exoerythrocytic forms (EEFs) were detected as early as 1 day postinfection, and larger EEFs were observed at later time points (Figures 2A and 2B). Furthermore, at 3 days postinfection the *P. berghei* (*P.b.*) EEFs expressed the mature EEF marker, MSP-1 (Figure 2C), suggesting that *P.b.* EEF maturation occurred along with *P.b.* EEF growth. In addition, separate cultures of iHLCs were infected with an alternate rodent *Plasmodium* species, *P. yoelii* (*P.y.*), and were shown to support *P.y.* EEFs that also increased in size over a 48 hr period postinfection (Figures 2D and 2E). iHLCs were next tested for their capacity to be infected by the human malaria parasite, *P. falciparum* (*P.f.*), and were found to harbor HSP70-expressing *P.f.* EEFs at 3 days postexposure (Figure 2F). Moreover, at 6 days postexposure, *P.f.* EEFs also expressed the liver-stage maturation marker, *P.f.* MSP-1 (Figure 2G; 10%–35% *P.f.* EEFs, as compared to 45% for *P.b.* EEFs), and increased in size compared to those observed at 3 days postexposure to *P.f.* sporozoites (Figures 2F and 2H). In addition to *P.f.*, iHLCs were also infected with sporozoites of a different human malaria species, *P. vivax* (*P.v.*), and were found to support HSP70-expressing *P.v.* EEFs that also increased in size from an average of 5 μm at 3 days postinfection to a wide range of sizes up to 77 μm by 8 days postinfection (Figures 2I and 2J). These results indicate that iHLC infectibility with *Plasmodium* sporozoites is not restricted to the rodent malaria species, and that the in-vitro-derived host cells can also support EEF maturation. Last, differentiated iHLCs were phenotypically stable and could be infected with *P.f.* sporozoites up to day 55 after initiation of differentiation (Figure S1 available online), which was the latest time point tested for *Plasmodium* infectibility in this study.

Kinetics of Acquisition of Permissiveness to *Plasmodium* Infectibility

To determine at what point in the 20 day in vitro differentiation process that iPSC-derived hepatic lineage cells become susceptible to malaria infection, cells at different stages of differentiation (iPS cells, endoderm, hepatic-specified endoderm, hepatoblast, iHLCs) were exposed to sporozoites obtained from a single batch of *P.f.*-infected *A. gambiae* mosquitoes. At 4 days postinfection, no *P.f.* EEFs were observed in iPSCs, whereas a small

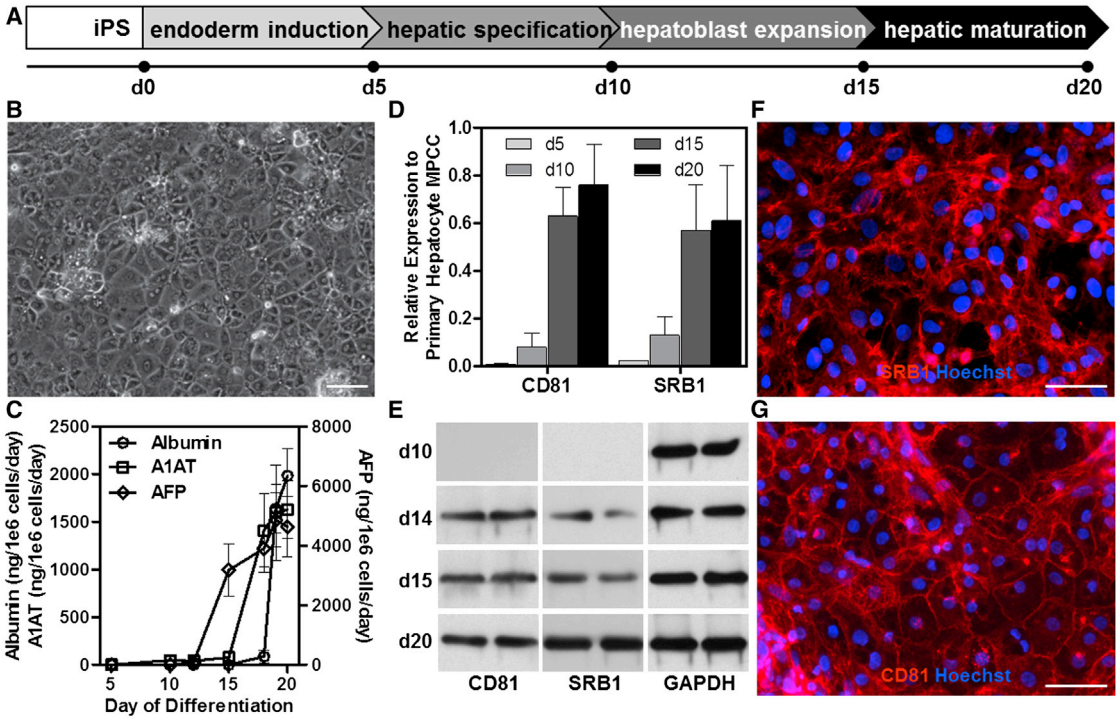

Figure 1. Characterization of iHLCs Derived by In Vitro Differentiation of iPSCs

(A) Schematic of protocol for the in vitro differentiation of iPS cells to iHLCs.

(B) Representative bright-field image showing typical hepatic morphology of iHLCs at d20 postdifferentiation.

(C) Kinetics of human albumin, α1-anti-trypsin (A1AT), and α-fetoprotein (AFP) secretion over the course of differentiation from iPS cells to iHLCs. n = 3 biological replicates per condition. Data are represented as mean ± SEM.

(D) Representative RT-PCR analysis of *CD81* and *SRB1* gene expression over the course of differentiation from iPS cells to iHLCs. n = 3 biological replicates per condition. Data are represented as mean ± SEM.

(E) Representative western blot analysis of CD81 and SRB1 protein expression over the course of differentiation from hepatic-specified endoderm cells to iHLCs. n = 2 biological replicates are shown.

(F and G) Representative immunofluorescence images of d20 iHLCs expressing (F) CD81 and (G) SRB1.

Scale bars, 50 μm.

number were observed in endoderm cells (d5 cells) and hepatic-specified endoderm cells (d10 cells) (Figures 3A and 3B). However, the number of *P.f.* EEFs was significantly higher in hepatoblasts (d15 cells) than in hepatic-specified endoderm cells and the frequency of infection remained elevated in differentiated iHLCs (d20 cells) (Figures 3A and 3B). Although some variability is observed between experiments regarding the relative number of *P.f.* EEFs observed between d15 and d20 cells (Figure 3B, left versus right), likely a product of the established stochastic nature of the iHLC differentiation process and also a function of heterogeneity of iPSC-derived progeny in each well, we consistently observed acquisition of more robust *P.f.* susceptibility between days 10 and 15 of the directed differentiation protocol. Notably, the size distributions of observed *P.f.* EEFs at 4 days postinfection were not significantly different at any time point (d5, d10, d15, d20 postdifferentiation) (Figure 3C), suggesting that the rare cells that exhibit permissiveness to *Plasmodium* sporozoite infection at earlier time points were already capable of supporting parasite survival and growth for at least 4 days postinfection. This pattern is emphasized by the observations at 6 days postinfection that d15 hepatoblasts maintained similar levels of *P.f.* infection as d20 iHLCs (Figure S2A), exhibited increased *P.f.* EEF sizes than at 4 days postinfection (Figure S2B), and supported the maturation of *P.f.* EEFs as demonstrated by the expression of the liver-stage maturation marker, *P.f.* MSP-1 (Figures S2A and S2C), and the appearance of merosome-like structures (Figure S2D). However, a higher proportion of *P.f.* EEFs in d20 iHLCs express *P.f.* MSP1 (~40%) than those in d15 hepatoblasts (~20%) (Figure S2A), and the *P.f.* EEF size distribution is larger in iHLCs than in hepatoblasts (Figure S2B) at 6 days postinfection. These data suggest that, whereas hepatoblasts are also capable of supporting *P.f.* EEF

survival, growth, and maturation, *P.f.* EEFs in hepatoblasts may develop to either a slower or smaller degree than those in iHLCs. In addition to their capacity to be infected by *P.f.* sporozoites, d16 hepatoblasts and completely differentiated iHLCs both support similar numbers of *P.y.* EEFs at 2 days postinfection (Figure S2E), suggesting that incompletely differentiated hepatoblasts have also acquired sufficient host factors to allow the invasion and growth of rodent *Plasmodium* sporozoites.

Plasmodium-Infected iHLCs Are Sensitive to Atovaquone but Not Primaquine

Because iHLCs obtained via the current iPSC in vitro differentiation protocol express a relatively low level of 83 human hepatic drug metabolism enzymes (DMEs) compared to primary human hepatocytes (Shan et al., 2013), we hypothesized that *Plasmodium*-infected iHLCs may only respond to antimalarial drugs that are active in their parent form, such as atovaquone (Biagini et al., 2012), and not to drugs that require bioactivation by hepatic DMEs in order to demonstrate inhibitory activity against the *Plasmodium* liver stages, such as primaquine (Bennett et al., 2013; Pybus et al., 2013). Indeed, when iHLCs infected with *P. yoelii* sporozoites were treated with 10 nM atovaquone or 10 μM primaquine starting at 3 hr postinfection, only the atovaquone-treated cultures were blocked in their ability to support *P.y.* EEFs (Figure 4A). In contrast, no differences in the number or size distribution of *P.y.* EEFs were observed in primaquine-treated iHLCs infected at either 23 or 28 days postdifferentiation (Figures 4B and 4C), suggesting that primaquine exposure had no impact on the infection or growth of *P.y.* EEFs. This finding supports the hypothesis that, whereas iHLCs support *P.y.* invasion and *P.y.* EEF growth, they do not express the appropriate hepatic DMEs, and/or other host factors, necessary for the bioactivation of primaquine into a form that can inhibit liver-stage *P.y.* EEFs. To confirm that the absence of primaquine sensitivity of *Plasmodium*-infected iHLCs extends to the human *Plasmodium* species, iHLCs were infected with *P. falciparum* sporozoites, and primaquine treatment was started 3 hr postexposure to sporozoites. As observed following infection with *P.y.*, primaquine treatment of *P.f.*-infected iHLCs did not reduce the number of *P.f.* EEFs (Figure 4D), nor did it alter the *P.f.* EEF size distribution (Figure 4E).

Small Molecule-Mediated Maturation of iHLCs Confers Primaquine Sensitivity

In order to utilize iHLCs in antimalarial phenotypic drug screens, it would be highly advantageous to obtain iHLCs with a developmentally mature hepatic DME profile. A previous high-throughput small molecule screen identified two small molecules capable of promoting transcriptional upregulation of many adult human hepatic DMEs (Shan et al., 2013), including the four DMEs CYP2D6, CYP3A4, CYP2C19, and MAO-A, that are responsible for the majority of primaquine metabolism and bioactivation in hepatocytes (Jin et al., 2014; Pybus et al., 2012, 2013). To test whether maturation of iHLCs induced by of these small molecules, FPH1, confers primaquine sensitivity, iHLCs were treated with either FPH1 or the DMSO carrier for a total of 6 days (treatment phase, D21–26). The iHLCs were cultured for an additional 1–2 days without the small molecule (washout phase, D27–28) before being exposed to *Plasmodium* sporozoites, in order to avoid any direct effects of the small molecule or DMSO on sporozoite infectivity, or on eventual drug sensitivity during the liver-stage infection (Figure 5A).

For the purposes of a moving toward an eventual high-throughput screening protocol, we used a bioluminescent strain of *P. yoelii* that expresses firefly luciferase (*P.y.-luc*) to readout parasite infection and growth in the presence of primaquine following FPH1-induced maturation of iHLCs. The bioluminescence of *P.y.-luc* liver-stage EEFs is directly proportional to the total liver-stage load, as measured by RT-PCR (Miller et al., 2013; Mwakingwe et al., 2009), and is also a function of the total number of EEFs per well and the mean EEF diameter in that well (Figure S3). Although *P.y.-luc* infection (as measured by BLI) in DMSO-treated iHLCs did not decrease upon primaquine treatment, iHLCs pretreated with FPH1 exhibited significantly lower levels of *P.y.-luc* infection (Figure 5B).

To determine whether primaquine sensitivity was also achieved in *P. falciparum*-infected iHLCs, iHLCs were pretreated with FPH1 or DMSO and exposed to *P.f.* sporozoites. At 4 days postinfection, the infected cultures were fixed, and *P.f.* infection was quantified by manual counts of *P.f.* EEFs immunostained for PfHSP70. As predicted, iHLCs pretreated with DMSO supported an equivalent number and size distribution of *P.f.* EEFs in the presence or absence of primaquine during infection. However, iHLCs pretreated with FPH1 exhibited a significant decrease in the number of *P.f.* EEFs present when infected in the presence of primaquine (Figure 5C). Furthermore, the fewer *P.f.* EEFs observed in FPH1 pretreated iHLCs showed a significant decrease in their size distribution (Figure 5D). Collectively, the data clearly show that primaquine becomes more effective against both *P. yoelii* and *P. falciparum* EEFs in cells exposed to FPH1.

DISCUSSION

In this study, we show the feasibility of infecting iHLCs with *P. berghei*, *P. yoelii*, *P. falciparum*, and *P. vivax*.

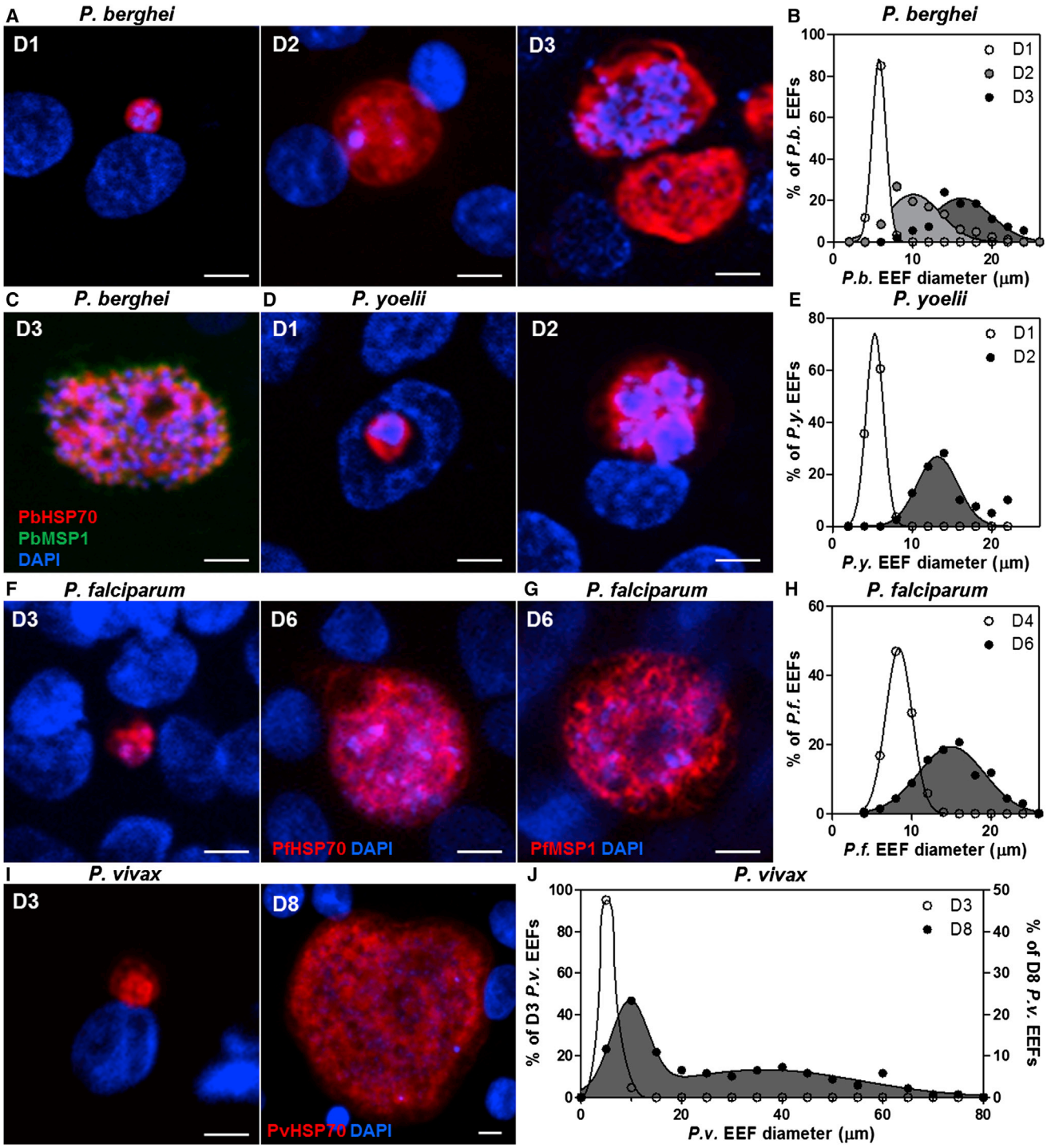

Figure 2. iHLCs Are Susceptible to Liver-Stage *Plasmodium* Infection

(A and B) (A) Representative immunofluorescence images of *P. berghei* (*P.b.*) EEFs and (B) *P.b.* EEF size distributions at D1, D2, or D3 postinfection in iHLCs.

(C) Representative immunofluorescence image of MSP1-positive *P.b.* EEF at D3 postinfection.

(D and E) (D) Representative immunofluorescence images of *P. yoelii* (*P.y.*) EEFs and (E) *P.y.* EEF size distributions at D1 or D2 postinfection in iHLCs.

(legend continued on next page)

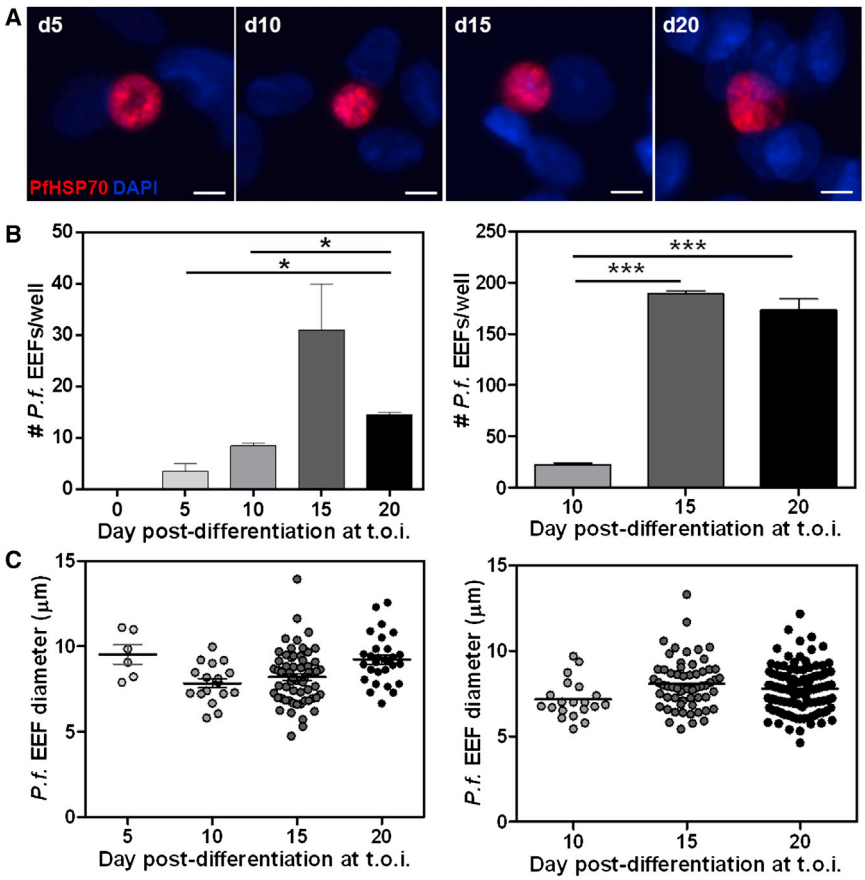

Figure 3. Kinetics of Acquisition of Permissiveness to *Plasmodium* Infectibility

(A) Representative IF images of *P. falciparum* (*P.f.*) EEFs from cells infected at various stages after the initiation of iPSC differentiation at D4 postinfection. Scale bars, 5 μm.

(B) Peak susceptibility to *P.f.* infection is attained at d15 after the initiation of differentiation, at the hepatoblast stage. The left and right panels represent two separate experiments using iHLCs from the same line but two separate differentiations, which were infected with two separate batches of *P.f.* sporozoites. n = 3 biological replicates per condition. Data are represented as mean ± SEM.

(C) Size distributions of *P.f.* EEFs obtained from an infection of cells at the endoderm (d5), hepatic-specified endoderm (d10), hepatoblast (d15), or iHLC (d20) stage.

*p < 0.05, ***p < 0.001; one-way ANOVA with Tukey's multiple comparison test. See also Figure S2.

Liver-stage *Plasmodium* EEFs grow in size over time and express MSP-1, which is typically expressed in more mature EEFs. Although iPS cells and definitive endoderm cells are generally not infectible with *P. falciparum*, some degree of *P. falciparum* infectibility is acquired by the time the cells are further differentiated to a hepatic-specified endoderm lineage. Notably, populations of hepatoblasts are equally or more infectible than the resulting iHLCs at the end of the in vitro differentiation protocol. iHLCs generated by the existing differentiation protocol do not respond to primaquine, a malaria drug that requires bioactivation by mature hepatic cytochrome P450 (CYP450) enzymes. However, further maturation of iHLCs using a previously described small molecule results in the acquisition of primaquine sensitivity, such that the drug treatment diminished infection by *P. yoelii* and *P. falciparum*.

In the context of drug development, there has been a shift from the traditional paradigm of testing drugs in immortalized cell lines to the use of primary cells, which have been increasingly recognized to offer better physiological relevance to drug screening and disease modeling in vitro (Engle and Puppala, 2013). A key goal of early-stage drug discovery platforms is the elimination of drug candidates that generate toxic metabolites that can cause drug-induced liver injury (DILI), a key cause of drug removal from the market (McDonnell and Braverman, 2006). To this end, a hepatic cell type that accurately recapitulates the native cellular physiology of an adult human hepatocyte is advantageous, but most hepatic cell lines lack the expression of a wide array of such key adult hepatic metabolism activity (March et al., 2013) because they are largely tumor derived (i.e., HepG2) or tumor associated

(F and H) (F) Representative immunofluorescence images of *P. falciparum* (*P.f.*) EEFs and (H) *P.f.* EEF size distributions at D3 or D6 postinfection in iHLCs.

(G) Representative immunofluorescence image of MSP1-positive *P.f.* EEF at D6 postinfection.

(I and J) (I) Representative immunofluorescence images of *P. vivax* (*P.v.*) EEFs and (J) *P.v.* EEF size distributions at D3 or D8 postinfection in iHLCs.

Scale bars, 5 μm. See also Figure S1.

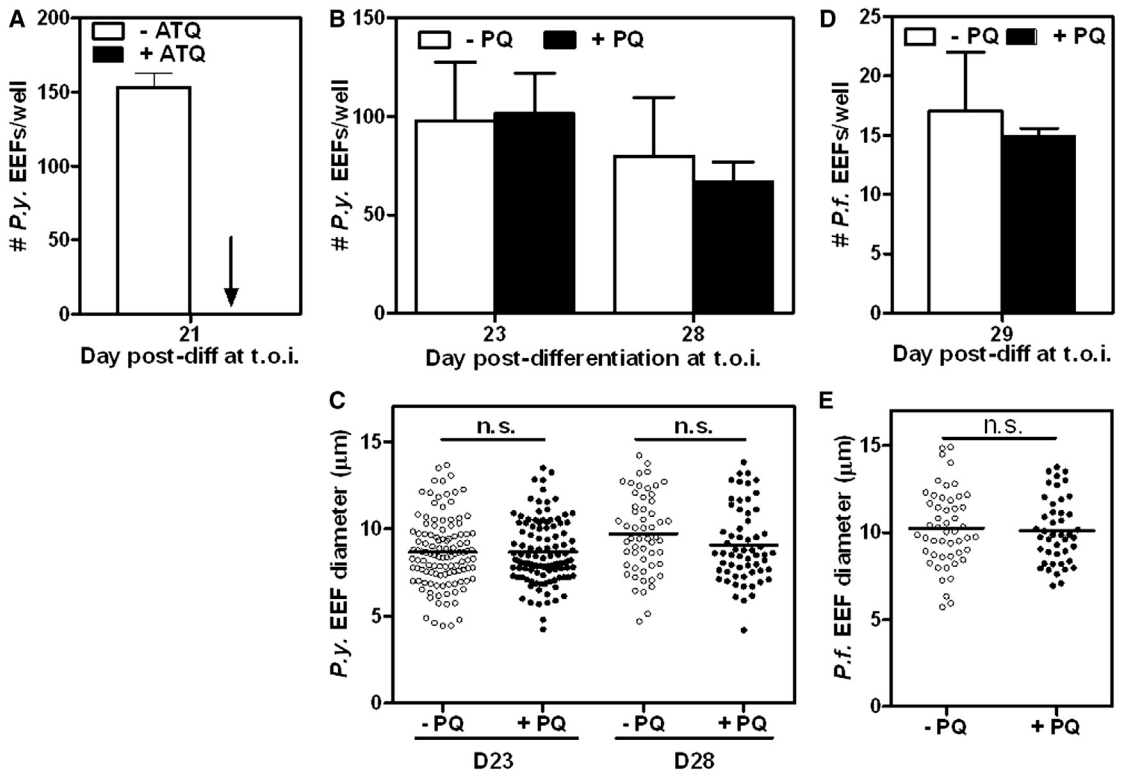

Figure 4. *Plasmodium*-Infected iHLCs Are Sensitive to Atovaquone but Not Primaquine

(A) Number of *P. yoelii* (*P.y.*) EEFs per well in iHLCs that were infected at 21 days postdifferentiation in the presence or absence of 10 nM atovaquone (ATQ). n = 3 biological replicates per condition.

(B and C) (B) Number of *P.y.* EEFs per well and (C) size distributions of *P.y.* EEFs in iHLCs that were infected at 23 or 28 days postdifferentiation in the presence or absence of 10 μM primaquine (PQ). n = 3 biological replicates per condition.

(D and E) (D) Number of *P. falciparum* (*P.f.*) EEFs per well and (E) size distributions of *P.f.* EEFs in iHLCs that were infected at 29 days postdifferentiation in the presence or absence of 10 μM primaquine.

n = 3 biological replicates per condition. Two-tailed t test run for panels (B)–(E). Data are represented as mean ± SEM.

(i.e., HC04). A second major goal of drug discovery platforms is the ability to identify nontoxic compounds that demonstrate differential efficacy in a phenotypic screen relevant to a disease. In the case of drug discovery against the malarial liver stages, it is therefore highly advantageous to utilize a cell type that best represents the primary adult hepatocyte. At the same time, it is also ideal to represent highly polymorphic genetic variants in drug metabolism and different ethnic groups in such drug screens, as these factors may influence the efficacy of potential antimalarial drug candidates. For example, genetic polymorphisms in CYP2D6 metabolism that stratified *P. vivax* patients into poor, intermediate, or extensive CYP2D6 metabolizers were recently reported to correlate with the risk of a failure of primaquine to prevent malaria relapse due to *P. vivax* (Bennett et al., 2013). Several cell sources have been proposed to augment the genetic variation and supply of adult primary human hepatocytes, including xenogenic or fetal human tissue, or embryonic stem cell-derived hepatocytes, but these sources are hampered by safety, ethical, or sourcing issues.

iPSC-derived iHLCs offer a unique advantage in that they can be generated from any donor, which allows a broad spectrum of the human population to be represented in in vitro drug screens and provides an opportunity to assess donor-specific drug responses in vitro. Recent collaborations between drug discovery companies and academic laboratories (Engle and Puppala, 2013) mark the development of an infrastructure that will benefit future personalized models of human diseases, including hepatotropic diseases like the relapsing forms of malaria.

iPSCs can also be engineered using DNA editing techniques to incorporate any genetic abnormality or modification to enable the exploration of the role that host genetics plays in liver-stage malaria infection. Although clinically relevant host factors that influence hepatic susceptibility to liver-stage malaria infection have not been documented, the study of potential host factors may benefit from the

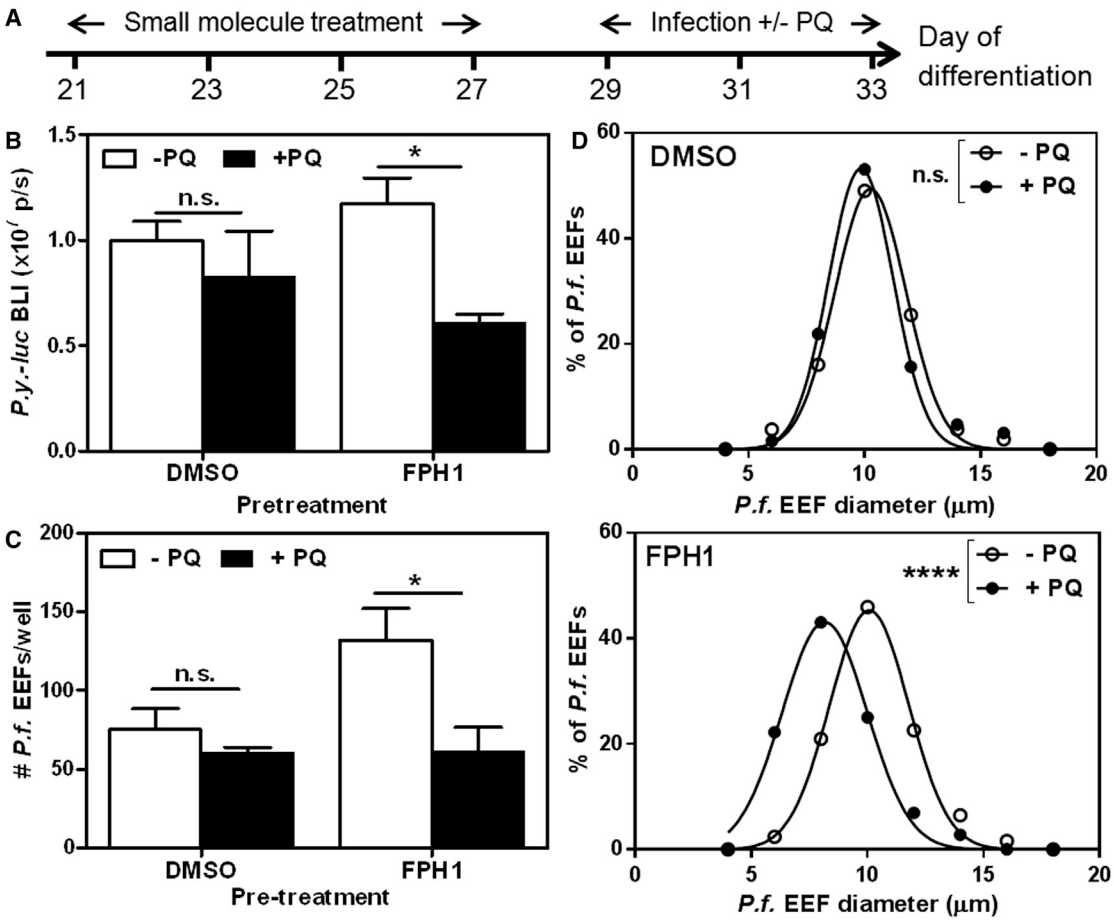

Figure 5. Small Molecule-Mediated Maturation of iHLCs Confers Primaquine Sensitivity

(A) Schematic of small molecule dosing of iHLCs before infection with *P. yoelii-luciferase* (*P.y.-luc*) or *P. falciparum* (*P.f.*).

(B) Effect of FPH1 pretreatment on primaquine (PQ) sensitivity (closed bars, 10 μM primaquine) of iHLCs infected with *P.y.-luc*. Infection was measured by bioluminescence imaging of *P.y.-luc*-infected iHLCs. n = 4 biological replicates per condition. *p < 0.05, two-tailed t test. See also Figure S3.

(C) Effect of FPH1 pretreatment on primaquine sensitivity of iHLCs infected with *P.f.* Infection was measured by counting the number of *P.f.* EEFs per well. n = 4 biological replicates per condition. *p < 0.05, two-tailed t test.

(D) Size distributions of *P.f.* EEFs in *P.f.*-infected iHLCs that were pretreated with the DMSO carrier or FPH1 and treated with or without 10 μM primaquine after infection. ****p < 0.0001, two-tailed t test. Data are represented as mean ± SEM.

larger pool of genetic variation that is accessible with the use of iPSCs. This effort may have implications in drug discovery against the liver stages of malaria species that present with large genetic heterogeneities in different parts of the world, especially the relapsing malaria species like *P. vivax* (e.g., temperate versus tropical strains), which may have coevolved to infect geographically distinct human populations (Cui et al., 2003; Dondorp et al., 2009; Gunawardena et al., 2010; Li et al., 2001).

From a developmental standpoint, the infectibility of iHLCs with liver-stage malaria and other hepatotropic pathogens such as the hepatitis viruses could also be a potential biomarker of hepatic lineage commitment, with iPSCs becoming permissive only when they become sufficiently hepatocyte-like. The ability to study liver-stage malaria infection at different developmental stages during the in vitro directed differentiation of iPSCs into iHLCs within a single donor may also facilitate the identification of host factors required for permissiveness to *Plasmodium* sporozoite infection and the elucidation of the roles that these host factors play in malaria pathogenesis.

One potential measure of how developmentally close iHLCs are to primary human hepatocytes is the efficiency of liver-stage malaria infection of iHLCs compared to primary human hepatocytes. With the multiplicity of infection (MOI) of approximately 0.5 used in the above

P. falciparum experiments (with respect to the estimated number of iHLCs per well based on an estimate of differentiation efficiency), an infection rate of approximately 0.3–1.8 *P.f.* EEFs per 10,000 iHLCs is obtained. In comparison, a microscale human liver platform that was recently reported to support *P. falciparum* infection in primary human hepatocytes reported an infection rate of approximately 100 *P.f.* EEFs per 10,000 hepatocytes at 3.5 days after infection with an MOI of 15 (March et al., 2013). Assuming that the infection rate scales linearly with MOI for the purposes of this analysis, an MOI of 0.5 in primary human hepatocytes would be estimated to give rise to an infection rate of approximately 3 *P.f.* EEFs per 10,000 hepatocytes. This suggests that iHLCs exhibit anywhere from 10%–60% of the infectibility of primary human hepatocytes and indicates that iHLCs have acquired sufficient hepatocyte-like characteristics that confer infectibility with liver-stage malaria.

The observation that iHLCs are infectible with malaria before their in vitro differentiation is complete could reflect the acquisition of some liver-stage malaria host entry factors during the iPSC differentiation process, or heterogeneity in iPSC differentiation that results in faster hepatic maturation of a subpopulation of cells. This observation could also suggest the possibility of some promiscuity in the host entry factors that are required for *Plasmodium* sporozoite entry. Further studies are required to determine whether the EEFs observed in incompletely differentiated iPSCs reflect fully replication-competent EEFs, or whether such EEFs are prone to developmental arrest due to the absence (or presence) of some host factor that promotes (or inhibits) parasite development. It is intriguing that hepatoblasts appear to support similar *P. falciparum* infection rates and similar degrees of parasite growth as iHLCs, with some experiments even exhibiting a trend of increased numbers of *P.f.* EEFs or *P.y.* EEFs in hepatoblasts compared to iHLCs (Figures 3B, left, and S2E). This slight difference in infectibility could suggest the acquisition of sufficient host entry factors that support *Plasmodium* infection and development by d15 postinitiation of differentiation from iPSCs, but that further maturation beyond the hepatoblast stage results in the acquisition of other host factors that henceforth limit EEF development and survival. Because the cells in different stages of in vitro differentiation arise from the same donor, these observations also offer a clean comparative system in which to systematically probe and identify host factors that are essential for liver-stage malaria parasite infections, using proteomics or gene expression technologies, in a donor-independent manner.

A common shortcoming of iHLCs and other iPSC-derived cells lies in the fact that they often resemble a developmentally immature state compared to the fully differentiated adult counterpart (Engle and Puppala, 2013). In the field of iHLCs, current in vitro differentiation protocols result in the production of a hepatic cell type that is biologically closer to fetal hepatocytes than adult hepatocytes, due to the incomplete abrogation of the expression of fetal markers such as alpha-fetal protein (AFP) (Si-Tayeb et al., 2010; Song et al., 2009), and the incomplete acquisition of an adult-like levels of key secretory, detoxification, and metabolic activity (Shan et al., 2013). Our data show that further chemical maturation of iHLCs allows the acquisition of primaquine sensitivity, presumably via the acquisition of a drug metabolism enzyme (DME) expression profile that better resembles the adult human hepatocyte. This advance decreases the biological gap between iHLCs and primary adult hepatocytes and increases the potential utility of iHLCs in drug development efforts for malaria and other diseases. The expression of a developmentally mature repertoire of hepatic DMEs is particularly important considering that current drug development efforts toward malaria eradication revolves around the 8-aminoquinoline family, which is currently the only class of drugs that is efficacious against the cryptic hypnozoite stage of *P. vivax* liver-stage infections (Wells et al., 2009), and the fact that many existing antimalarial drugs such as proguanil, artemether, lumefantrine, and halofantrine are known to undergo metabolism in the liver by hepatic DMEs (Khoo et al., 2005) and whose in vitro efficacy will therefore likely be predictive of in vivo efficacy only if the in vitro hepatocyte model exhibits a primary human hepatocyte DME expression profile. Although the primaquine response in iHLCs pretreated with FPH1 was incomplete, other primary human hepatocyte models of *P. falciparum* treated with the same primaquine concentration (10 μM) also exhibit an incomplete response, with about 10%–20% of the number of *P.f.* EEFs remaining (Dembele et al., 2011; March et al., 2013). An unexpected finding was that FPH1 pretreatment also increased the baseline number of *P.f.* EEFs in iHLCs in the absence of primaquine treatment compared to DMSO pretreatment (Figure 5C). The chemical maturation of iHLCs by FPH1 is likely to involve a complex mechanism, which could theoretically result either in an increase in the adult hepatic phenotype of the existing population of iHLCs and hence their infectibility by *Plasmodium* sporozoites, or an expansion in the population of iHLCs or of other hepatic progenitors. Chemically matured iHLCs with increased baseline infectibility with *Plasmodium* could therefore provide an opportunity to elucidate hepatic host factors that promote liver-stage malaria infection in hepatocytes.

In conclusion, the establishment of *Plasmodium* liver-stage infections in induced pluripotent stem cell-derived hepatocyte-like cells lays the foundation for their use in antimalarial drug discovery as well as paves the way to study the genetic basis of host-*Plasmodium* interactions.

EXPERIMENTAL PROCEDURES

iPSC Culture and Hepatocyte-like Cell Generation

Undifferentiated iPSC were maintained and differentiated into iHLCs as described (Si-Tayeb et al., 2010). In brief, iPSCs were cultured in monolayer on Matrigel (Becton Dickinson), and directed differentiation was achieved by sequential exposure to activin A, bone morphogenic protein 4, basic FGF, HGF, and oncostatin M (OSM). For *P. berghei* and *P. yoelii* experiments, iHLCs differentiated from the iPSC lines, RC2 (reprogrammed from fibroblasts by the laboratory of Darrell Kotton at Boston University) (Somers et al., 2010), iPS.C2a (reprogrammed from foreskin fibroblasts by the laboratory of Stephen Duncan at Medical College of Wisconsin) (Si-Tayeb et al., 2010), or LN4 (a subclone of iPS.C2a with higher uniformity in growth and differentiation) were used. For *P. falciparum* experiments, iHLCs differentiated from the iPSC line, LN4, or cryopreserved iHLCs from Cellular Dynamics International (white female donor, iPSCs reprogrammed from fibroblasts, iCell Hepatocytes 2.0, CDI) were used. For *P. vivax* experiments, cryopreserved iHLCs (white female donor, iPSCs reprogrammed from fibroblasts, or white male donor, iPSCs reprogrammed from peripheral blood mononuclear cells, iCell Hepatocytes 2.0, CDI) were used. Cryopreserved iHLCs from CDI were thawed, plated on collagen I, and maintained according to the manufacturer's instructions until used.

Sporozoites

P. berghei ANKA and *P. yoelii* sporozoites were obtained by dissection of the salivary glands of infected *Anopheles stephensi* mosquitoes obtained from the insectaries at New York University or Harvard School of Public Health. *P. falciparum* sporozoites were obtained by dissection of the salivary glands of infected *Anopheles gambiae* mosquitoes obtained from the insectary at Johns Hopkins School of Public Health. *P. vivax* sporozoites were kindly provided by the insectary at Mahidol Vivax Research Center (Bangkok, Thailand) and were prepared by dissection of the salivary glands of infected *Anopheles dirus* mosquitoes.

Infection of iHLCs

P. berghei, *P. yoelii*, *P. falciparum*, or *P. vivax* sporozoites from dissected mosquito glands were centrifuged at 600 × *g* for 5 min on to iHLCs at a multiplicity of infection of 0.1–1 in the presence of 2% fetal bovine serum. After incubation at 37°C and 5% CO_2 for 2–3 hr, the wells were washed twice before serum-free culture medium was added. Media was replaced daily. Samples were fixed 24, 48, or 65 hr postinfection with *P. berghei* and *P. yoelii*, 3, 4, or 6 days postinfection with *P. falciparum*, and 3 or 8 days postinfection with *P. vivax*. For *P. vivax* experiments, iHLCs from CDI were exposed to *P. vivax* sporozoites at 4 days postplating.

Immunofluorescence Assay

iHLCs were fixed with −20°C methanol for 10 min at 4°C, washed thrice with PBS, blocked with 2% BSA in PBS overnight at 4°C, and then incubated overnight at 4°C with a primary antibody: mouse anti-human CD81 (clone JS-81, BD Pharmingen; 1:200), rabbit anti-SRB1 (Novus Biologicals; 1:100), mouse anti-PbHSP70 (clone 2E6; 1:200 for *P. berghei* and *P. yoelii*), rabbit anti-PbMSP1 (1:500 for *P. berghei*), mouse anti-PfHSP70 (clone 4C9, Sanaria; 1:200 for *P. falciparum*), or mouse anti-PfMSP1 (1:200 for *P. falciparum*). Samples were washed thrice with PBS before incubation for 1–3 hr at room temperature with secondary antibody: goat anti-mouse Alexa Fluor 594 or Alexa Fluor 488 or donkey anti-rabbit-Alexa Fluor 488 (Invitrogen; 1:400). Nuclei were then counterstained with Hoechst 33258 (Invitrogen; 1:1000), samples were washed thrice with PBS, and 1 ml of Aquamount (Thermo-Scientific) was added per well. Images were captured on a Nikon Eclipse Ti fluorescence microscope or an Olympus FV1000 multiphoton laser scanning confocal microscope.

Biochemical Assays

Cell culture supernatants were collected and stored at –20°C. Human albumin, α1-anti-trypsin (A1AT), and α-fetoprotein (AFP) secretion were measured by enzyme-linked immunosorbent assays with horseradish peroxidase detection (Bethyl Labs) and 3,3′,5,5′-tetramethylbenzidine (TMB, Pierce) development.

Statistics

Experiments were repeated with three or more independent batches of differentiated iHLCs with triplicate or quadruplicate biological samples for each condition. Data from representative batches of iHLCs are presented. Two-tailed t tests were performed for all comparisons between two conditions (e.g., with or without primaquine). One-way ANOVAs were performed for comparisons involving three or more conditions (e.g., number of EEFs in cells infected at various time points after differentiation) with Tukey's post hoc test for multiple comparisons. All error bars represent SEM.

SUPPLEMENTAL INFORMATION

Supplemental Information includes three figures and can be found with this article online at http://dx.doi.org/10.1016/j.stemcr.2015.01.002.

AUTHOR CONTRIBUTIONS

S.N., R.E.S., S.M., and S.N.B. designed experiments. S.N., S.M., A.G., and N.G. performed malaria experiments. R.E.S. and M.P. generated and characterized iHLCs. S.N. and S.N.B. analyzed data. S.N. and S.N.B. wrote the manuscript.

ACKNOWLEDGMENTS

We thank Ana Rodriguez and Sandra Gonzalez (New York University) for providing mosquitoes infected with *P. yoelii* and *P. berghei*, Dyann Wirth and Emily Lund (Harvard School of Public Health) for providing mosquitoes infected with *P. berghei*, Photini Sinnis and Abhai Tripathi (Johns Hopkins Bloomberg School of Public Health) for providing mosquitoes infected with *P. falciparum*, Jetsumon Sattabongkot Prachumsri and Rapatbhorn Patrapuvich (Mahidol University) for providing fresh *P. vivax* sporozoites, Cellular Dynamics International (CDI) for providing iCell Hepatocytes 2.0 for *P. vivax* experiments, Jeffrey B. Wyckoff (Koch Institute, MIT) for technical help in confocal microscopy, Stephen Duncan (Medical College of Wisconsin) for iPS cell lines and counsel on iHep generation, and Heather Fleming for critical reading and

help with manuscript preparation. This work was supported by the Bill and Melinda Gates Foundation (award number 51066). S.N. is supported by an A*STAR (Agency for Science, Technology and Research, Singapore) National Science Scholarship, US National Institutes of Health (NIH) grant UH3-EB017103, and in part by the Koch Institute Support (core) Grant P30-CA14051 from the National Cancer Institute. S.N.B. is a Howard Hughes Medical Institute Investigator.

Received: August 11, 2014
Revised: January 4, 2015
Accepted: January 5, 2015
Published: February 5, 2015

REFERENCES

Bennett, J.W., Pybus, B.S., Yadava, A., Tosh, D., Sousa, J.C., McCarthy, W.F., Deye, G., Melendez, V., and Ockenhouse, C.F. (2013). Primaquine failure and cytochrome P-450 2D6 in Plasmodium vivax malaria. N. Engl. J. Med. *369*, 1381–1382.

Biagini, G.A., Fisher, N., Shone, A.E., Mubaraki, M.A., Srivastava, A., Hill, A., Antoine, T., Warman, A.J., Davies, J., Pidathala, C., et al. (2012). Generation of quinolone antimalarials targeting the Plasmodium falciparum mitochondrial respiratory chain for the treatment and prophylaxis of malaria. Proc. Natl. Acad. Sci. USA *109*, 8298–8303.

Cui, L., Escalante, A.A., Imwong, M., and Snounou, G. (2003). The genetic diversity of Plasmodium vivax populations. Trends Parasitol. *19*, 220–226.

da Cruz, F.P., Martin, C., Buchholz, K., Lafuente-Monasterio, M.J., Rodrigues, T., Sönnichsen, B., Moreira, R., Gamo, F.-J., Marti, M., Mota, M.M., et al. (2012). Drug screen targeted at Plasmodium liver stages identifies a potent multistage antimalarial drug. J. Infect. Dis. *205*, 1278–1286.

Dembele, L., Gego, A., Zeeman, A.-M., Franetich, J.-F., Silvie, O., Rametti, A., Le Grand, R., Dereuddre-Bosquet, N., Sauerwein, R., van Gemert, G.-J., et al. (2011). Towards an in vitro model of Plasmodium hypnozoites suitable for drug discovery. PLoS ONE *6*, e18162.

Derbyshire, E.R., Prudêncio, M., Mota, M.M., and Clardy, J. (2012). Liver-stage malaria parasites vulnerable to diverse chemical scaffolds. Proc. Natl. Acad. Sci. USA *109*, 8511–8516.

Dondorp, A.M., Nosten, F., Yi, P., Das, D., Phyo, A.P., Tarning, J., Lwin, K.M., Ariey, F., Hanpithakpong, W., Lee, S.J., et al. (2009). Artemisinin resistance in Plasmodium falciparum malaria. N. Engl. J. Med. *361*, 455–467.

Engle, S.J., and Puppala, D. (2013). Integrating human pluripotent stem cells into drug development. Cell Stem Cell *12*, 669–677.

Gunawardena, S., Karunaweera, N.D., Ferreira, M.U., Phone-Kyaw, M., Pollack, R.J., Alifrangis, M., Rajakaruna, R.S., Konradsen, F., Amerasinghe, P.H., Schousboe, M.L., et al. (2010). Geographic structure of Plasmodium vivax: microsatellite analysis of parasite populations from Sri Lanka, Myanmar, and Ethiopia. Am. J. Trop. Med. Hyg. *82*, 235–242.

Jin, X., Pybus, B.S., Marcsisin, R., Logan, T., Luong, T.L., Sousa, J., Matlock, N., Collazo, V., Asher, C., Carroll, D., et al. (2014). An LC-MS based study of the metabolic profile of primaquine, an 8-aminoquinoline antiparasitic drug, with an in vitro primary human hepatocyte culture model. Eur. J. Drug Metab. Pharmacokinet. *39*, 139–146.

Khoo, S., Back, D., and Winstanley, P. (2005). The potential for interactions between antimalarial and antiretroviral drugs. AIDS *19*, 995–1005.

Li, J., Collins, W.E., Wirtz, R.A., Rathore, D., Lal, A., and McCutchan, T.F. (2001). Geographic subdivision of the range of the malaria parasite Plasmodium vivax. Emerg. Infect. Dis. *7*, 35–42.

March, S., Ng, S., Velmurugan, S., Galstian, A., Shan, J., Logan, D.J., Carpenter, A.E., Thomas, D., Sim, B.K.L., Mota, M.M., et al. (2013). A microscale human liver platform that supports the hepatic stages of Plasmodium falciparum and vivax. Cell Host Microbe *14*, 104–115.

Mazier, D., Rénia, L., and Snounou, G. (2009). A pre-emptive strike against malaria's stealthy hepatic forms. Nat. Rev. Drug Discov. *8*, 854–864.

McDonnell, M.E., and Braverman, L.E. (2006). Drug-related hepatotoxicity. N. Engl. J. Med. *354*, 2191–2193, author reply 2191–2193.

Meister, S., Plouffe, D.M., Kuhen, K.L., Bonamy, G.M., Wu, T., Barnes, S.W., Bopp, S.E., Borboa, R., Bright, A.T., Che, J., et al. (2011). Imaging of Plasmodium liver stages to drive next-generation antimalarial drug discovery. Science (80-.). *334*, 1372–1377.

Miller, J.L., Murray, S., Vaughan, A.M., Harupa, A., Sack, B., Baldwin, M., Crispe, I.N., and Kappe, S.H.I. (2013). Quantitative bioluminescent imaging of pre-erythrocytic malaria parasite infection using luciferase-expressing Plasmodium yoelii. PLoS ONE *8*, e60820.

Mwakingwe, A., Ting, L.-M., Hochman, S., Chen, J., Sinnis, P., and Kim, K. (2009). Noninvasive real-time monitoring of liver-stage development of bioluminescent Plasmodium parasites. J. Infect. Dis. *200*, 1470–1478.

Ogawa, S., Surapisitchat, J., Virtanen, C., Ogawa, M., Niapour, M., Sugamori, K.S., Wang, S., Tamblyn, L., Guillemette, C., Hoffmann, E., et al. (2013). Three-dimensional culture and cAMP signaling promote the maturation of human pluripotent stem cell-derived hepatocytes. Development *140*, 3285–3296.

Prudêncio, M., Rodriguez, A., and Mota, M.M. (2006). The silent path to thousands of merozoites: the Plasmodium liver stage. Nat. Rev. Microbiol. *4*, 849–856.

Pybus, B.S., Sousa, J.C., Jin, X., Ferguson, J.A., Christian, R.E., Barnhart, R., Vuong, C., Sciotti, R.J., Reichard, G.A., Kozar, M.P., et al. (2012). CYP450 phenotyping and accurate mass identification of metabolites of the 8-aminoquinoline, anti-malarial drug primaquine. Malar. J. *11*, 259.

Pybus, B.S., Marcsisin, S.R., Jin, X., Deye, G., Sousa, J.C., Li, Q., Caridha, D., Zeng, Q., Reichard, G.A., Ockenhouse, C., et al. (2013). The metabolism of primaquine to its active metabolite is dependent on CYP 2D6. Malar. J. *12*, 212.

Schwartz, R., Trehan, K., Andrus, L., Sheahan, T.P., Ploss, A., Duncan, S.A., Rice, C.M., and Bhatia, S.N. (2012). Modeling hepatitis C

virus infection using human induced pluripotent stem cells. Proc. Natl. Acad. Sci. USA *109*, 2544–2548.

Schwartz, R.E., Fleming, H.E., Khetani, S.R., and Bhatia, S.N. (2014). Pluripotent stem cell-derived hepatocyte-like cells. Biotechnol. Adv. *32*, 504–513.

Shan, J., Schwartz, R.E., Ross, N.T., Logan, D.J., Thomas, D., Duncan, S.A., North, T.E., Goessling, W., Carpenter, A.E., and Bhatia, S.N. (2013). Identification of small molecules for human hepatocyte expansion and iPS differentiation. Nat. Chem. Biol. *9*, 514–520.

Shlomai, A., Schwartz, R.E., Ramanan, V., Bhatta, A., de Jong, Y.P., Bhatia, S.N., and Rice, C.M. (2014). Modeling host interactions with hepatitis B virus using primary and iPSC-derived hepatocellular systems. Proc. Natl. Acad. Sci. USA *111*, 12193–12198.

Si-Tayeb, K., Noto, F.K., Nagaoka, M., Li, J., Battle, M.A., Duris, C., North, P.E., Dalton, S., and Duncan, S.A. (2010). Highly efficient generation of human hepatocyte-like cells from induced pluripotent stem cells. Hepatology *51*, 297–305.

Somers, A., Jean, J.-C., Sommer, C.A., Omari, A., Ford, C.C., Mills, J.A., Ying, L., Sommer, A.G., Jean, J.M., Smith, B.W., et al. (2010). Generation of transgene-free lung disease-specific human induced pluripotent stem cells using a single excisable lentiviral stem cell cassette. Stem Cells *28*, 1728–1740.

Song, Z., Cai, J., Liu, Y., Zhao, D., Yong, J., Duo, S., Song, X., Guo, Y., Zhao, Y., Qin, H., et al. (2009). Efficient generation of hepatocyte-like cells from human induced pluripotent stem cells. Cell Res. *19*, 1233–1242.

Takahashi, K., Tanabe, K., Ohnuki, M., Narita, M., Ichisaka, T., Tomoda, K., and Yamanaka, S. (2007). Induction of pluripotent stem cells from adult human fibroblasts by defined factors. Cell *131*, 861–872.

Takayama, K., Inamura, M., Kawabata, K., Katayama, K., Higuchi, M., Tashiro, K., Nonaka, A., Sakurai, F., Hayakawa, T., Furue, M.K., and Mizuguchi, H. (2012). Efficient generation of functional hepatocytes from human embryonic stem cells and induced pluripotent stem cells by HNF4α transduction. Mol. Ther. *20*, 127–137.

Takebe, T., Sekine, K., Enomura, M., Koike, H., Kimura, M., Ogaeri, T., Zhang, R.-R., Ueno, Y., Zheng, Y.-W., Koike, N., et al. (2013). Vascularized and functional human liver from an iPSC-derived organ bud transplant. Nature *499*, 481–484.

Thomson, J. a. (1998). Embryonic Stem Cell Lines Derived from Human Blastocysts. Science (80-.). *282*, 1145–1147.

Wells, T.N.C., Alonso, P.L., and Gutteridge, W.E. (2009). New medicines to improve control and contribute to the eradication of malaria. Nat. Rev. Drug Discov. *8*, 879–891.

World Health Organization (2013). World malaria report 2013.

Stem Cell Reports, Volume *4*

Supplemental Information

Human-Induced Pluripotent Stem Cell-Derived Hepatocyte-like Cells Support *Plasmodium* Liver-Stage Infection In Vitro

Shengyong Ng, Robert E. Schwartz, Sandra March, Ani Galstian, Nil Gural, Jing Shan, Mythili Prabhu, Maria M. Mota, and Sangeeta N. Bhatia

Human Induced Pluripotent Stem Cell-Derived Hepatocyte-like Cells Support *Plasmodium* Liver Stage Infection *In Vitro*

Shengyong Ng[1], Robert E. Schwartz[2,3], Sandra March[2,6], Ani Galstian[2,6], Nil Gural[2], Jing Shan[2], Mythili Prabhu[2], Maria M. Mota[5], Sangeeta N. Bhatia[2,3,5,6]

Supplemental Data

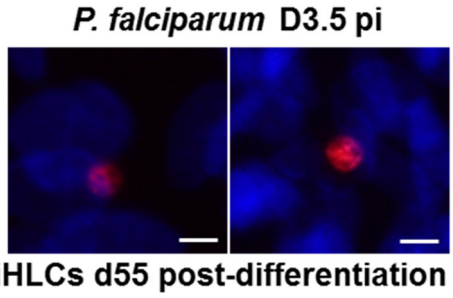

Figure S1, Related to Figure 2. Long-term maintenance of infectibility with *P. falciparum* in iHLCs. Representative IF images of *P. falciparum* EEFs at D3.5 post-infection in iHLCs at d55 post-differentiation, or 35 days after differentiation was completed. Scale bars = 5 μm.

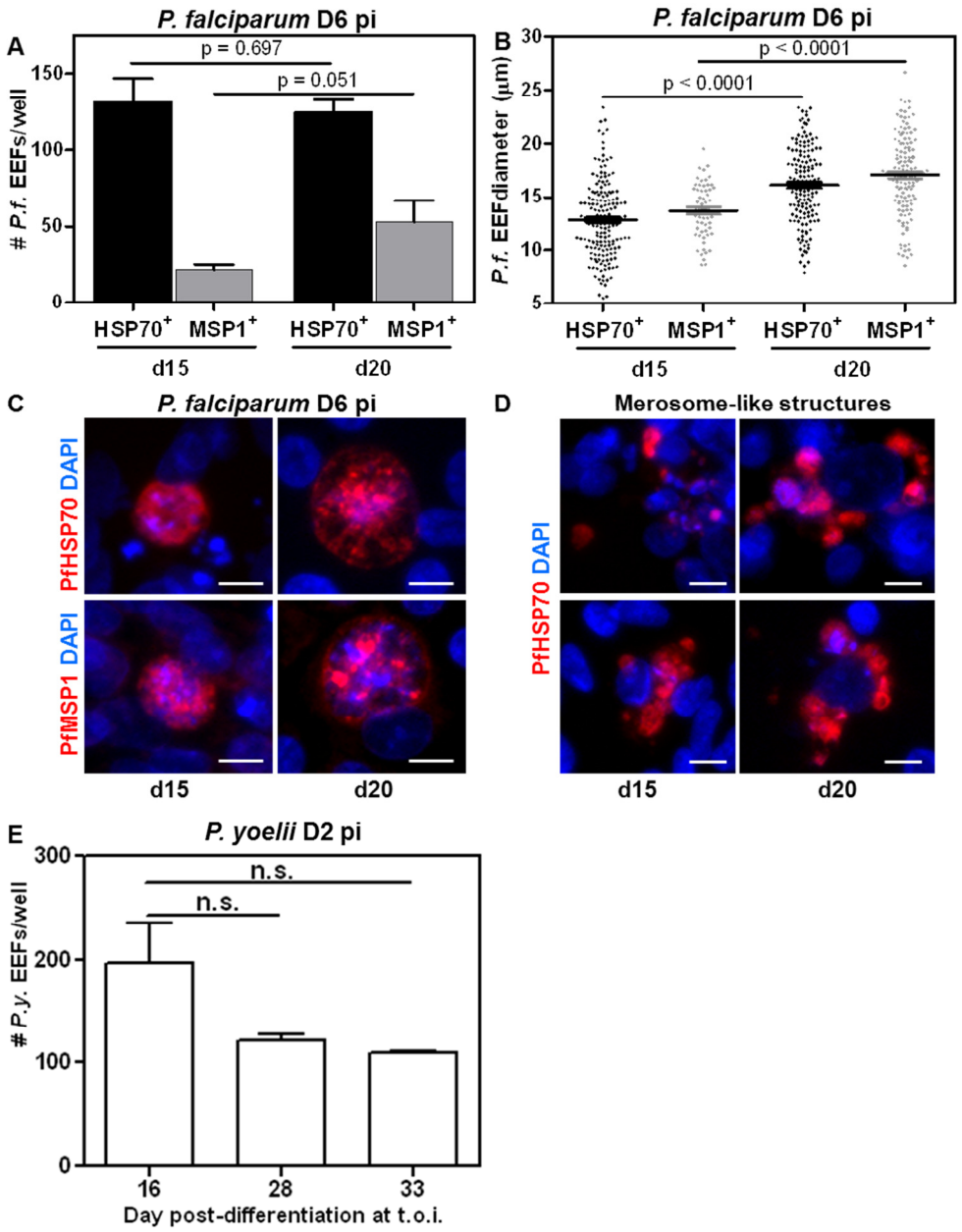

Figure S2, Related to Figure 3. Hepatoblasts and iHLCs support late-stage *P. yoelii* and *P. falciparum* infections. (A) Total number of *P.f.* EEFs (HSP70$^+$) and number of mature MSP1$^+$ *P.f.* EEFs at D6 post-infection in hepatoblasts (d15) and iHLCs (d20). n = 3 biological replicates per condition. (B) Size distributions of *P.f.* EEFs at D6 post-infection in hepatoblasts and iHLCs. (C) Representative immunofluorescence images of HSP70$^+$ or MSP1$^+$ *P.f.* EEFs at D6 post-infection in hepatoblasts and iHLCs. (D) Representative immunofluorescence images of merosome-like structures at D6 post-infection in hepatoblasts and iHLCs. (E) Number of *P.y.* EEFs at D2 post-infection in cells infected at various time points (d16, d28, d33) after the start of the

differentiation process. d16 cells are hepatoblasts, whereas d28 and d33 cells are iHLCs. n = 3 biological replicates per condition. Data are represented as mean ± SEM. Scale bars = 10 μm.

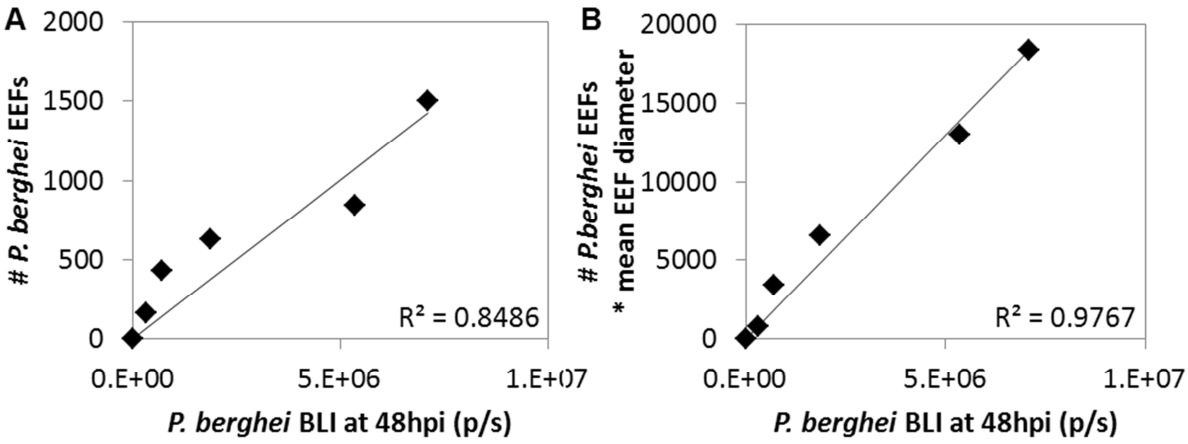

Figure S3, Related to Figure 5. Bioluminescent *Plasmodium* strains are a good proxy of total parasite load. Luciferase-expressing *P. berghei* (*P.b.*) sporozoites were added to different wells of iHLCs from the same batch of differentiation, and the infection was imaged in an IVIS bioluminescence (BLI) imaging system at 48h post-infection. A range of BLI values were obtained, suggesting a range of infection levels was obtained. The samples were fixed and stained for PbHSP70, and the number of *P.b.* EEFs in each well was counted. In addition the sizes of about 50 randomly chosen EEFs in each well were quantified by ImageJ. (A) shows the correlation between the number of *P.b.* EEFs versus the *P.b.* BLI, whereas (B) shows the correlation between the product of the number of *P.b.* EEFs and the mean EEF diameter versus the *P.b.* BLI.